Increased Fibulin-5 and Elastin in S100A4/Mts1 Mice With Pulmonary Hypertension

Sandra L. Merklinger, Roger A. Wagner, Edda Spiekerkoetter, Aleksander Hinek, Russell H. Knutsen, M. Golam Kabir, Kavin Desai, Shelby Hacker, Lingli Wang, Gordon M. Cann, Noona S. Ambartsumian, Eugene Lukanidin, Daniel Bernstein, Mansoor Husain, Robert P. Mecham, Barry Starcher, Hiromi Yanagisawa, Marlene Rabinovitch

Abstract—Transgenic mice overexpressing the calcium binding protein, S100A4/Mts1, occasionally develop severe pulmonary vascular obstructive disease. To understand what underlies this propensity, we compared the pulmonary vascular hemodynamic and structural features of S100A4/Mts1 with control C57Bl/6 mice at baseline, following a 2-week exposure to chronic hypoxia, and after 1 and 3 months "recovery" in room air. S100A4/Mts1 mice had greater right ventricular systolic pressure and right ventricular hypertrophy at baseline, which increased further with chronic hypoxia and was sustained after 3 months "recovery" in room air. These findings correlated with a heightened response to acute hypoxia and failure to vasodilate with nitric oxide or oxygen. S100A4/Mts1 mice, when compared with C57Bl/6 mice, also had impaired cardiac function judged by reduced ventricular elastance and decreased cardiac output. Despite higher right ventricular systolic pressures with chronic hypoxia, S100A4/Mts1 mice did not develop more severe PVD, but in contrast to C57Bl/6 mice, these features did not regress on return to room air. Microarray analysis of lung tissue identified a number of genes differentially upregulated in S100A4/Mts1 versus control mice. One of these, fibulin-5, is a matrix component necessary for normal elastin fiber assembly. Fibulin-5 was localized to pulmonary arteries and associated with thickened elastic laminae. This feature could underlie attenuation of pulmonary vascular changes in response to elevated pressure, as well as impaired reversibility. (***Circ Res*****. 2005;97:596-604.)**

Key Words: elastin ■ fibulin-5 ■ hypoxia ■ mouse ■ pulmonary hypertension ■ smooth muscle cells ■ S100 proteins ■ vascular smooth muscle cells ■ vascular disease

Familial idiopathic pulmonary arterial hypertension (PAH) is associated with mutations in bone morphogenetic receptor II (BMPR-II), but the inheritance pattern is that of a dominant gene with low penetrance, in that only ≈20% of affected family members develop the disease.[1,2] This coupled to the fact that genetically engineered mice with abnormalities in BMPR-II have pulmonary hypertension but fail to reproduce the pathology seen in patients with pulmonary vascular obstructive disease (PVD)[3,4] indicates that multiple genetic and environmental cofactors may be necessary for the disease to develop. A potential modifier gene is the calcium-binding protein, S100A4/Mts1, because a small subpopulation (≈5%) of transgenic mice >1 year of age, that overexpress S100A4/Mts1, develops PVD.[5] Furthermore, heightened expression of S100A4/Mts1 is observed in the neointima and adventitia of occlusive and early plexiform lesions in patients with a congenital heart defect or idiopathic PAH.[5] S100A4/Mts1 is induced in malignant metastatic breast cancer[6] and although its intracellular properties have been implicated in the motility of cancer cells,[7] it is also secreted and can stimulate angiogenesis.[8] Moreover, recombinant S100A4/Mts1 promotes proliferation and migration of cultured pulmonary artery (PA) SMC.[8a] Although these data suggest possible mechanisms underlying abnormal cellular responses associated with PVD in S100A4/Mts1 overexpressing mice, they do not address why the pathology only occurs in a small percentage of these animals. We hypothesized that other factors suppress the cellular effects of S100A4/Mts1 in the overexpressing mice, and that hypoxia-mediated vasoconstriction might derepress this protective mechanism. We therefore subjected S100A4/Mts1 and age- and gender-matched control C57Bl/6 background (nonlittermate) mice to

Original received February 3, 2005; resubmission received June 27, 2005; revised resubmission received August 1, 2005; accepted August 9, 2005.

From the Departments of Pediatrics (S.L.M., E.S., K.D., L.W., G.M.C., D.B., M.R.) and Medicine (R.A.W.), Stanford University School of Medicine, Calif; the Cardiovascular Research Program (A.H.), The Hospital for Sick Children, and the Department of Laboratory Medicine and Pathobiology and Center for Cardiovascular Research (M.G.K., M.H.), The Toronto Hospital Network, Division of Cardiology, Department of Medicine, University of Toronto, Canada; the Department of Medicine (R.H.K., R.P.M.), Washington University School of Medicine, St. Louis, Mo; the Department of Molecular Biology (S.H., H.Y.), University of Texas Southwestern Medical Center at Dallas; the Department of Molecular Cancer (N.S.A., E.L.), Institute of Cancer Biology, Danish Cancer Society, Copenhagen, Denmark; and the Department of Biomedical Research (B.S.), University of Texas Health Science Center at Tyler.

Correspondence to Dr Marlene Rabinovitch, The Vera Moulton Wall Center for Pulmonary Vascular Disease, Stanford University School of Medicine, CCSR Bldg, Room 2245a, 269 Campus Dr, Stanford, CA 94305-5162. E-mail marlener@stanford.edu

Circulation Research **is available at http://circres.ahajournals.org** **DOI: 10.1161/01. RES.0000182425.49768.8a**

2 weeks of hypoxia and also followed their "recovery" in room air for up to 3 months.

Materials and Methods

Experimental Design

Transgenic mice overexpressing S100A4/Mts1 (obtained from N.S.A. and E.L., Danish Cancer Society, Copenhagen, Denmark) were generated as described.[9] For chronic hypoxia, oxygen levels were maintained with the ProOx 110 system (BioSpherix) and carbon dioxide levels monitored continuously using the TelAire 7001 monitor (TelAire). All studies were performed under a protocol approved by the Animal Care Committee at Stanford University following the guidelines of the American Physiological Society.

Hemodynamic Measurements

Right ventricular systolic pressure (RVSP) was measured in nonventilated mice as described[10] and systemic blood pressure determined by direct carotid catheterization, both using the PowerLab/4SP recording unit (AD Instruments).

Right Ventricular Hypertrophy

Righte ventricular hypertrophy (RVH) was measured as described[10] by the weight of the right ventricle relative to body weight and relative to left ventricle+septum.

Morphometric Analysis

Transverse lung sections were stained by Movat pentachrome or with an alpha-smooth muscle actin antibody (DakoCytomation, Carpinteria, Calif). From all mice, we took the same full section in the mid-portion of the lung parallel to the hilum, and embedded it in the same manner. Muscularization was assessed by comparing fully and partially muscularized alveolar wall and duct arteries to total peripheral PAs. The total number of peripheral arteries was calculated as a ratio of number of arteries/100 alveoli in each field and verified using sections in which the endothelial cells were stained by an antibody to von Willebrand factor.[11] All morphometric analyses were performed by one blinded observer.

Cardiac Output Measurement

Cardiac output (CO) was assessed using a Siemens Sequoia C512 ultrasound machine and calculated by $([Pi \times (Aod)^2 \times VTI \times HR]/4)$, where Aod is aortic diameter, VTI is velocity time integral and HR is heart rate.

Micro CT Imaging

The eXplore Locus Micro CT Scanner (GE Medical Systems) was used to acquire nondestructing 3D images of barium-infused[12] whole lung specimens. The barium was infused by hand with similar gross and microscopic end points of precapillary filling of all small vessels at alveolar duct and wall level. Images were scanned at 45 μm resolution using eXplore Evolver software. Qualitative assessment of distal arborization was performed by 2 independent blinded observers. Left PA measurements were made using eXplore Reconstruction Utility software.

Pulmonary Vascular Reactivity

Continuous RVSP measurements were obtained in ventilated, anesthetized (1% to 2% isoflurane) mice at baseline (40% oxygen), during 5 minutes of acute hypoxia (10% oxygen), followed by the addition of inhaled nitric oxide (NO) (40ppm) for 5 minutes, and with return to 40% oxygen.

Vascular Compliance

Compliance measurements of the left-common carotid artery, left branch PA, and ascending aorta were made as previously described with assessments of external diameter of the vessel for each level of intravascular pressure applied.[13]

Ventricular Function (Elastance)

Ventricular elastance of anesthetized (1% to 2% isoflurane) mice was assessed as previously described[14] using the Aria System (Millar Instruments). Signals from the catheter were digitized using the Powerlab system and stored for offline analysis using the PVAN software (Pressure-Volume Analysis, Millar Instruments).

Microarray Analysis

Microarray studies of whole lung tissue, data acquisition, analysis, and statistical analysis were performed as previously described.[15]

Quantitative RT-PCR Analysis

RNA was extracted from mouse whole lung tissue or from human PA-SMCs by Trizol preparation. RNA was reverse-transcribed using Superscript II (Invitrogen) as per manufacturer's instructions. Gene expression levels were quantified using preverified Assays-on-Demand TaqMan primer/probe sets (Applied Biosystems). Expression level of each gene was normalized to 18S ribosomal RNA using the comparative delta-CT method.

Western Immunoblots for Fibulin-5 and S100A4/Mts1

Proteins were resolved on 4% to 12% Bis-Tris gels with a 1:100 concentration of the rabbit polyclonal antibody, BSYN1923, raised against rat fibulin-5 polypeptide (supplied by H.Y., University of Texas Southwestern Medical Center, Dallas) or a 1:2000 concentration of rabbit polyclonal S100A4/Mts1 antibody (supplied by N.S.A., Danish Cancer Society, Copenhagen, Denmark). The specificity of the antibody was determined by its failure to cross-react with other S100 proteins[5] and by negative immunostaining of sections from the knockout mice (unpublished observations). The specificity of the fibulin antibody is also evident by failure of immunodetection in the knockout mouse.[16] Normalization for protein was performed by reprobing the membrane with the control house-keeping gene, S6 (Cell Signaling Technology, Beverly, Mass).

Immunohistochemistry

Immunohistochemistry, using techniques previously described,[10] was performed on lung sections perfused with saline and fixed in 10% formalin. Polyclonal fibulin-5 antibody (1:100) and a species-specific secondary reagent were used based on the avidin-biotin peroxidase method (Vector Laboratories).

Cell Culture

Human PA SMCs (Cascade Biologics, Portland, Ore) were grown to 70% confluence and cultured for 48 hours in media with 0.1% serum before stimulation with recombinant S100A4/Mts1 (500 ng/mL; supplied by Drs Ambartsumian and Lukanidin) for 0, 1, 6, 12, 24, and 48 hours. Quantitative RT-PCR for fibulin-5 was performed as described above.

Electron Microscopy

Transmission EM was performed as described[17] and measurements of internal and external elastic laminae and medial width were made of PAs at the respiratory bronchiolus level. Assessments were made using Open Laboratory software (Improvision) of 5 to 10 separate images per sample acquired at equidistant points.

Elastin and Elastase Assays

To measure desmosine content in the tissues as a marker of insoluble elastin, the lungs at the hilum, the central pulmonary artery from pulmonary valve to bifurcation, and the thoracic aorta (top of the arch to the diaphragm) of control C57Bl/6 and Mts1 overexpressing mice were harvested. Tissues were hydrolyzed, and desmosine quantified by a ninhydrin based radioimmunoassay.[18] Values were related to total protein, to the tissue segment, and to body weight.[19] Elastase activity was measured in whole lung tissue by a modification of a method previously described[19] using fluorescein-conjugated

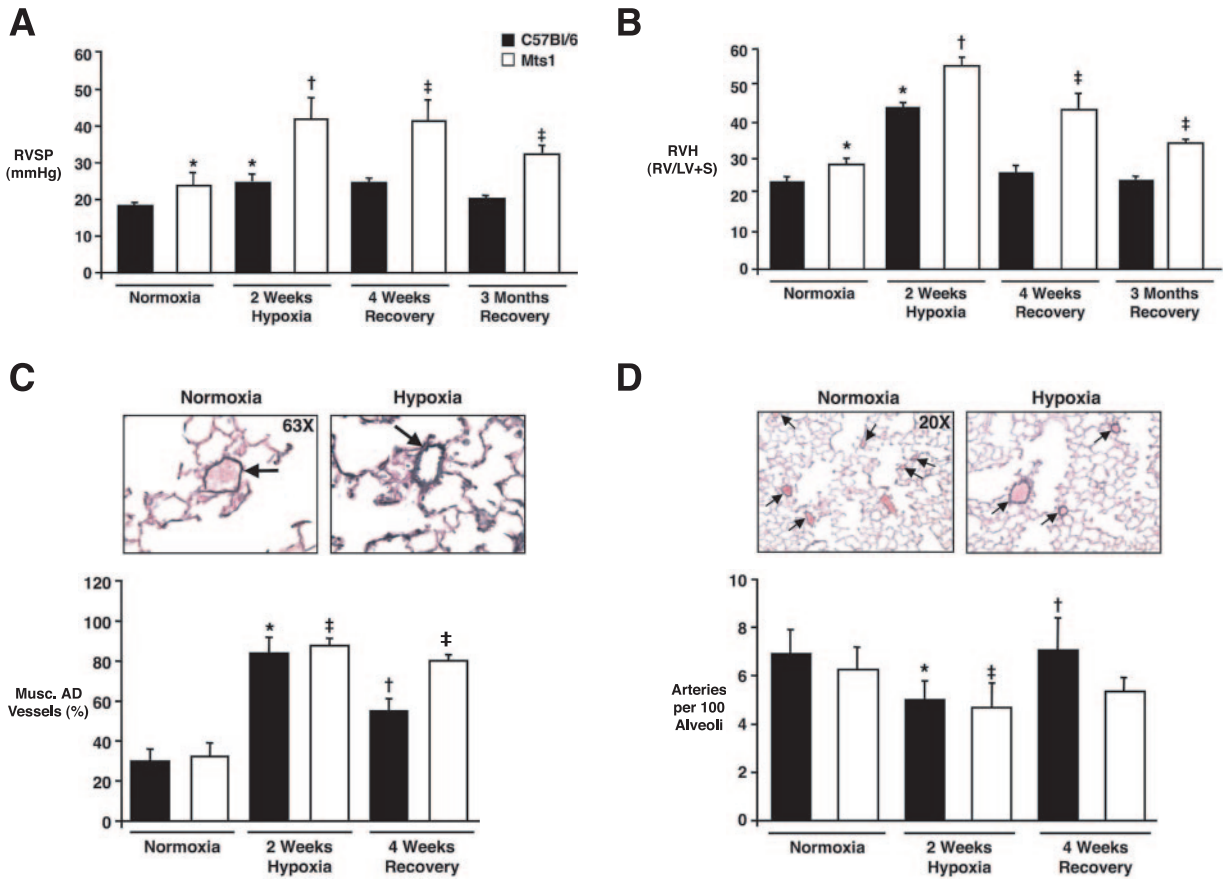

Figure 1. Pulmonary hypertension in S100A4/Mts1 mice. S100A4/Mts1 and control C57Bl/6 mice were exposed to hypoxia (10% oxygen) followed by room air "recovery" for 4 weeks and 3 months. Right ventricular systolic pressure (RVSP) measurements (A) and ratio of the weight of the right ventricle (RV) to that of left ventricle (LV) plus septum (B) as an index of right ventricular hypertrophy (RVH). C, Representative photomicrograph of lung tissue stained by Movat pentachrome showing a hypoxia-induced increase in arterial muscularization (upper) and graphic representation of the presence and degree of muscularization of alveolar duct Pas (lower). Arrows denote alveolar duct-associated arteries. D, Representative photomicrograph of lung tissue stained by Movat pentachrome showing a hypoxia-induced decrease in arterial number (upper) and morphometric analysis of fully and partially muscularized alveolar duct (AD) and wall PAs relative to 100 alveoli (lower). Arrows denote alveolar duct and wall arteries. Bars represent mean±SEM (A and B, n=12 to 20; C and D, n=8 to 12); *$P<0.05$ compared with C57Bl/6 normoxic mice; †$P<0.05$ compared with C57Bl/6 hypoxic mice; ‡$P<0.05$ compared with S100A4/Mts1 normoxic mice. (P values <0.05 are not distinguished to simplify the annotations.)

bovine neck ligament elastin (EnzChek Elastase Assay Kit, Molecular Probes, Eugene, Ore).

Statistical Analysis

Values from multiple experiments are expressed as mean±SEM. Statistical significance was determined using one-way analysis of variance followed by Fisher least significant difference test of multiple comparisons to establish differences between individual groups. A P value of <0.05 was considered as significant. The number of mice or samples in each group is indicated in the figure legends.

Results

Hemodynamic and Morphometric Assessments

We measured RVSP as an indication of pulmonary arterial pressure (PAP) and observed a mild elevation in the S100A4/Mts1 compared with C57Bl/6 mice under baseline room air conditions ($P<0.01$). Following 2 weeks of chronic hypoxia (10% oxygen), a greater elevation in RVSP was observed in the S100A4/Mts1 compared with the C57Bl/6 control mice. Moreover, in contrast to C57Bl/6 mice, the elevated RVSP in the S100A4/Mts1 mice did not regress even following return to room air for 3 months ($P<0.01$) (Figure 1A). In keeping with the elevation in RVSP, we also observed more severe right ventricular hypertrophy (RVH) in the S100A4/Mts1 versus C57Bl/6 mice that was sustained during room air recovery only in the S100A4/Mts1mice ($P<0.01$) (Figure 1B).

Despite the more severe elevation in RVSP and RVH at baseline and following hypoxia, S100A4/Mts1 and C57Bl/6 mice showed a similar degree of muscularization of distal vessels at alveolar duct and alveolar wall level and a similar reduction in the number of peripheral arteries at alveolar duct and wall level, calculated relative to 100 alveoli. This feature was confirmed using an antibody to von Willebrand factor to mark endothelial cells. However, consistent with the sustained elevation in RVSP in S100A4/Mts1 mice following return to room air, there was persistent muscularization of peripheral arteries ($P<0.02$) (Figure 1C), and a tendency for their number to remain reduced, compared with C57Bl/6 mice, in which values returned to normal levels (Figure 1D).

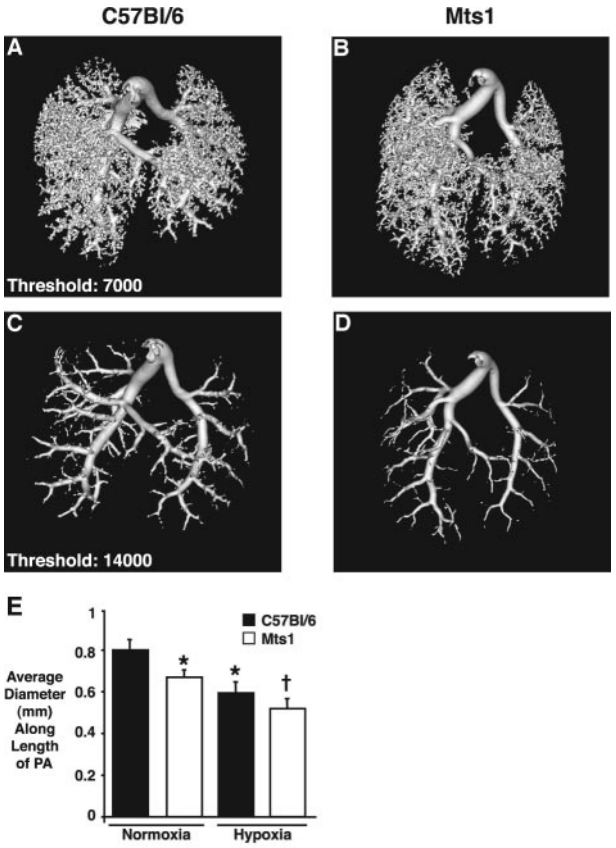

Figure 2. Micro CT imaging of barium-filled pulmonary arteries. Representative photomicrographs of micro CT images of whole lungs infused with barium gelatin from a C57Bl/6 (A) or a S100A4/Mts1 (B) mouse exposed to 2 weeks of hypoxia. 3D reconstructions of the pulmonary arterial trees were obtained using a threshold of 7000 arbitrary digital units. C and D, Images captured at a less sensitive threshold (14 000 arbitrary digital units). E, Direct diameter measurements along the length of the left PA from hilum to periphery in S100A4/Mts1 vs C57Bl/6 mice at baseline and after hypoxia. Diameters were obtained using the GE eXplore Reconstruction software. Bars represent mean±SEM (n=6); *$P<0.04$ compared with C57Bl/6 normoxic mice; †$P<0.02$ compared with Mts1 normoxic mice.

We observed no qualitative difference in pulmonary arterial arborization in 3D reconstruction of micro-computed tomography (CT) imaging of barium-infused lung samples comparing S100A4/Mts1 and control mice (Figure 2A and 2B). However, measurements of lumen diameter along the length of the left PA revealed reduced values in the S100A4/Mts1 mice versus C57Bl/6 animals in normoxia ($P<0.04$) (Figure 2C, 2D, and 2E). A similar hypoxia-induced reduction in lumen diameter was noted in both groups relative to normoxia controls ($P<0.04$ and 0.02 respectively).

The increase in RVSP in the S100A4/Mts1 versus C57Bl/6 mice at baseline was associated with a higher level of RVSP in response to acute hypoxia (10% oxygen for 5 minutes) ($P<0.01$), but a similar percent increase. However, S100A4/Mts1 mice showed no significant attenuation in RVSP in response to nitric oxide or 40% oxygen in contrast to the C57Bl/6 group where values returned to baseline levels (Figure 3A). There were no statistically significant differences in the compliance of the branch pulmonary artery of S100A4/Mts1 versus C57Bl/6 mice (Figure 3B) or in the other vessels studied (data not shown).

No significant difference in mean systemic arterial pressure was noted between the groups, and a comparable baseline and hypoxia-induced elevation in hematocrit value and reduction in body weight was observed. However, echocardiographic assessment revealed a reduced cardiac output (CO) in the S100A4/Mts1 versus C57Bl/6 mice both at baseline ($P<0.0001$) and following chronic hypoxia ($P<0.01$) (supplemental Table I, available online at http://circres.ahajournals.com). These results suggested that there was a greater elevation in pulmonary vascular resistance in the S100A4/Mts1 compared with C57Bl/6 mice.

Consistent with the reduced CO in the S100A4/Mts1 versus C57Bl/6 mice was a decrease in left ventricular function assessed by real-time continuous pressure-volume analysis of cardiac elastance[14] ($P<0.05$) (Figure 3C through 3E). End-diastolic pressure measurements were slightly higher in the S100A4/Mts1 versus C57Bl/6 mice ($P<0.05$) (supplemental Table II). Despite these indices of cardiac dysfunction that were measured under anesthesia, no frank evidence of heart failure judged by tachypnea or ascites, was observed in the S100A4/Mts1 mice at baseline or following hypoxia, and trichrome staining of heart tissue sections showed no increase in fibrosis relative to controls (data not shown).

Microarray Analysis of Lung Gene Expression

Differences in gene expression in S100A4/Mts1 versus control C57Bl/6 mice were assessed to explain the more severe PAH but relative attenuation of vascular disease during hypoxia, as well as the impaired regression following return to normoxia. There were 390 features exclusively upregulated in hypoxic S100A4/Mts1 versus C57Bl/6 mice, 226 known genes and 164 expressed sequence tags or poorly annotated features. A relatively smaller number of known genes, 147, were significantly upregulated in S100A4/Mts1 versus C57Bl/6 mice under normoxic conditions. Supplemental Table III summarizes some of the genes that were upregulated in S100A4/Mts1 versus C57Bl/6 mice under hypoxic conditions ($P<0.05$ for all comparisons) and selected for follow-up study for their functional relevance to vascular remodeling, eg, proteases, matrix components, growth and survival factors, or vasoreactive molecules. We were able to confirm significant elevation of the transcript in 2 of the 6 genes, and trends in 3 of the 6 by qRT-PCR. We also confirmed significant suppression of one transcript, bone morphogenetic protein receptor 1 (BMP-RI) by qRT-PCR (data not shown). We did not pursue the elevation in matrix metalloproteinase 2 in S100A4/Mts1 versus control mice during hypoxia, because the elevation in the activity of the enzyme by gelatin zymography was comparable in both groups in hypoxia relative to room air controls (data not shown).

Among the annotated genes that distinguished the S100A4/Mts1 from the C57Bl/6 mouse, only one, fibulin-5 (DANCE or EVEC), was significantly increased on microarray, both under normoxia and with chronic hypoxia. Fibulin-5, a calcium-dependent elastin-binding protein, is a necessary

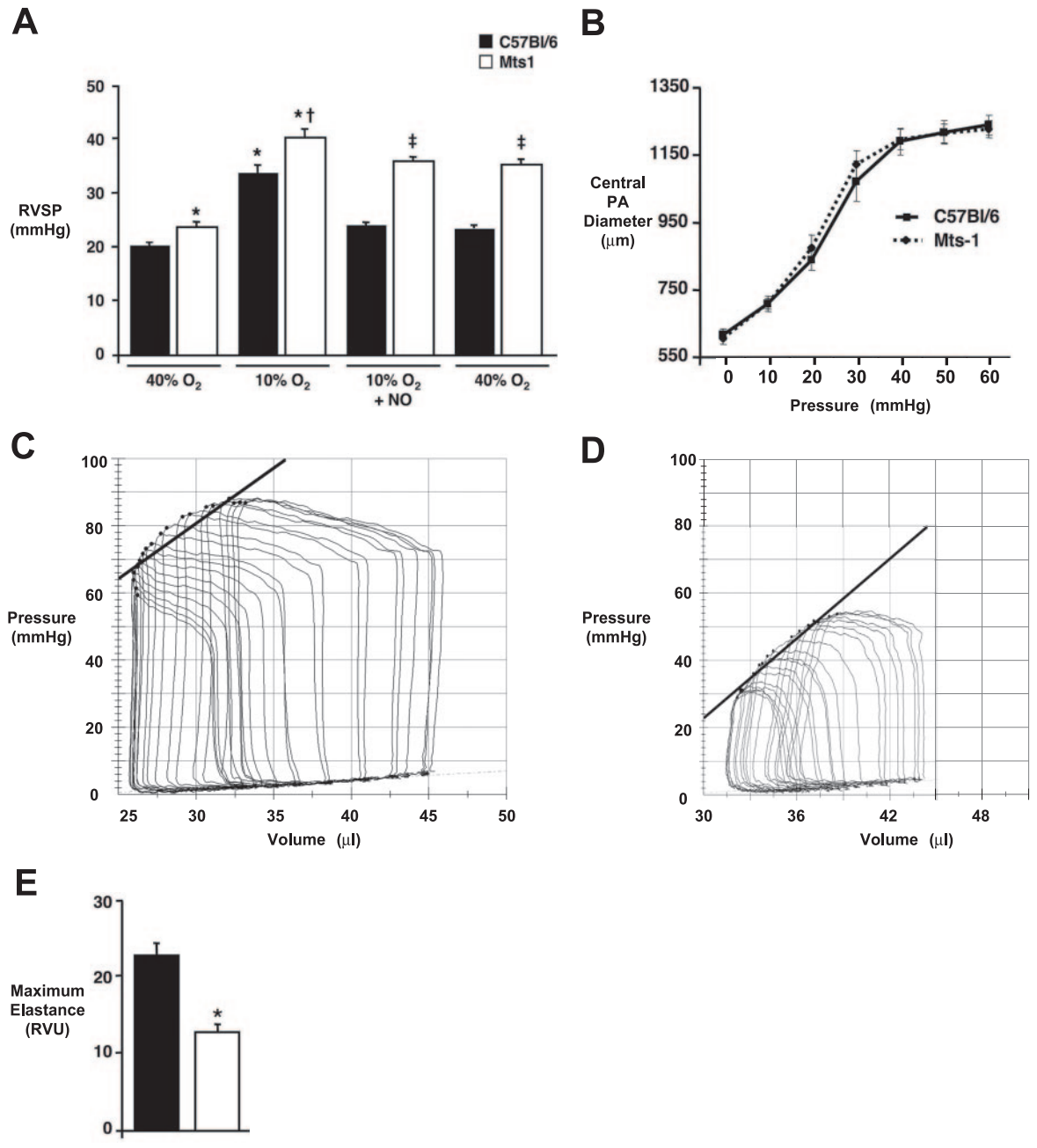

Figure 3. Vasoreactivity, arterial compliance ventricular elastance. A, RVSP measurements in S100A4/Mts1 vs C57Bl/6 mice at baseline (40% oxygen), during acute hypoxia (10% oxygen), hypoxia plus NO (40 ppm), and a return to 40% oxygen. B, Compliance measurements of the large arteries. Pressure-volume loops were made in C57Bl/6 (C) and S100A4/Mts1 (D) mice during baseline normoxic conditions. E, Maximum left ventricular elastance derived from the pressure-volume loop analysis was decreased in S100A4/Mts1 mice compared with C57Bl/6 animals. Bars represent mean±SEM, (A, C through E, n=8; B, n=6); *$P<0.05$ compared with C57Bl/6 normoxic mice; †$P<0.05$ compared with C57Bl/6 hypoxic mice; ‡$P<0.05$ compared with S100A4/Mts1 normoxic mice. (P values <0.05 are not distinguished to simplify the annotations.)

component of normal elastin fiber assembly.[16,20] We speculated that an increase in fibulin-5, could cause deposition of more elastin, altering the hemodynamic characteristics of the pulmonary vessel wall and also limit remodeling, particularly SMC proliferation.[21,22]

Fibulin-5 and Elastin

Analysis by qRT-PCR indicated only a trend toward heightened fibulin-5 mRNA expression in the lung at baseline and following hypoxia in S100A4/Mts1 versus C57Bl/6 control mice (Figure 4A). Densitometric analyses of the Western immunoblots of whole lung tissue, revealed a trend toward higher levels of fibulin-5 in S100A4/Mts1 versus C57Bl/6 mice in normoxia, but a significant difference between the groups in hypoxia ($P<0.03$) (Figure 4B). Although the data are not quantitative, we were able to localize heightened immunoreactivity for fibulin-5 to the PA muscular media as a consistent feature in vessels of different airway levels in S100A4/Mts1 versus C57Bl/6 mice in normoxia. Hypoxia per se appeared to induce a slight increase in fibulin-5 immuno-

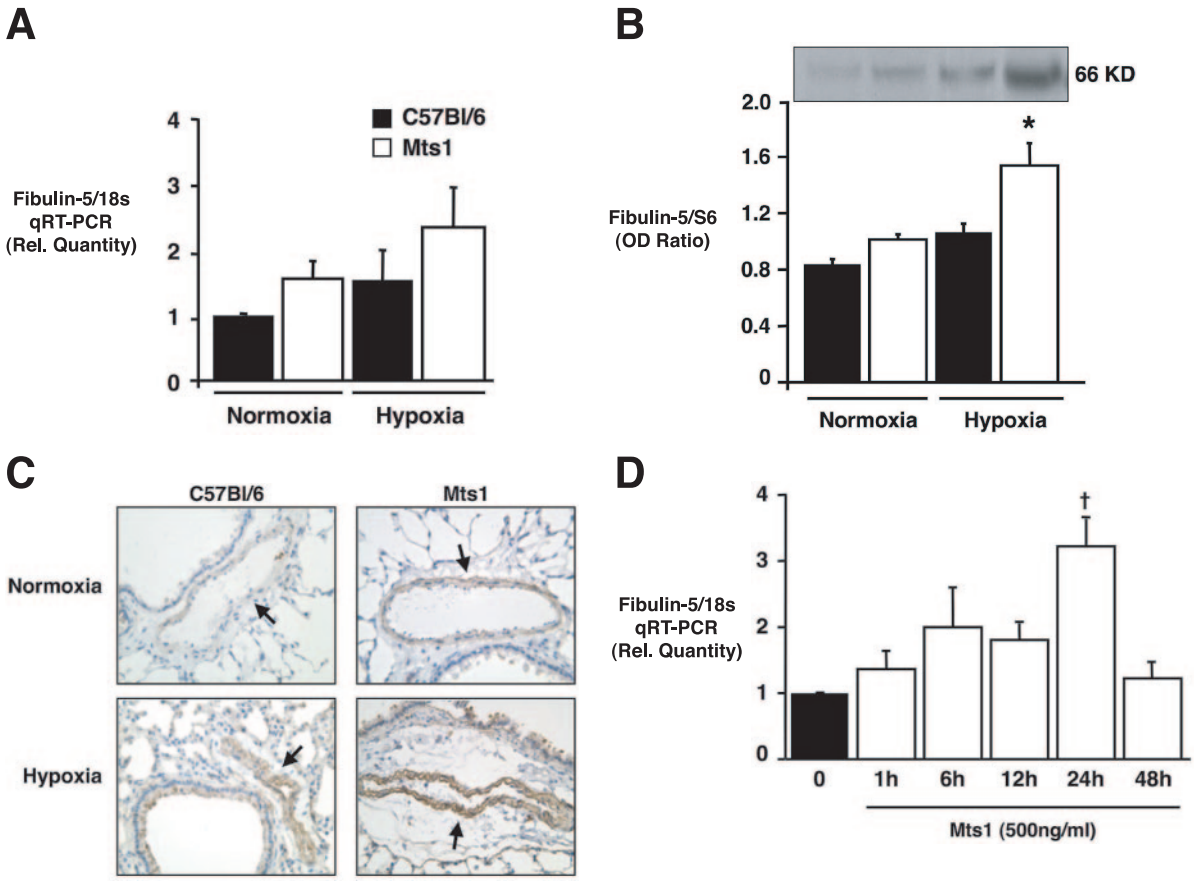

Figure 4. Fibulin-5 expression in S100A4/Mts1 mice and cultured pulmonary artery smooth muscle cells. A, Quantitative RT-PCR for fibulin-5mRNA in RNA from whole lung tissue of S100A4/Mts1 and C57Bl/6 mice exposed to room air or to 2 weeks of hypoxia. Expression levels of each gene were normalized to 18S ribosomal RNA and expressed as a fold change in gene expression compared with the control C57Bl/6 normoxic animals. B, Representative Western immunoblot showing expression of fibulin-5 protein in whole lung tissues of S100A4/Mts1 vs C57Bl/6 mice exposed to room air or hypoxia (top) and densitometric analysis of fibulin-5 protein, normalized to the internal housekeeping gene, S6, is shown in the bar graph (bottom). C, Representative photomicrographs of paraffin-embedded mouse lung tissue sections after immunoperoxidase staining for fibulin-5. Strong positive staining was noted particularly in the media of pulmonary arteries (arrows) of S100A4/Mts1 mice at baseline and after chronic hypoxia. D, Quantitative RT-PCR for fibulin-5mRNA in RNA extracted from human PA-SMCs stimulated with recombinant S100A4/Mts1 at indicated time points. Data represent mean±SEM, (A, C, and D, n=4; B, n=3); †$P<0.05$ compared with all groups. *$P<0.03$ vs C57BLl/6 hypoxia.

reactivity, a feature accentuated in the S100A4/Mts1 mice (Figure 4C). To determine whether S100A4/Mts1 could induce expression of fibulin-5, we incubated human PA-SMCs with recombinant S100A4/Mts1 for 48 hours and detected elevated fibulin-5 mRNA levels by qRT-PCR with a peak at 24 hours ($P<0.05$) (Figure 4D).

The elevation in fibulin-5 in S100A4/Mts1 versus C57Bl/6 mice, at baseline and following exposure to chronic hypoxia, was associated with increased thickness of the internal (Figure 5B) and external (Figure 5C) elastic laminae, as assessed by transmission EM in arteries at the level of the respiratory bronchiolus ($P<0.05$ for all comparisons). Moreover, an increase in medial width, associated with hypertrophy of the SMCs, was also noted in the hypoxic S100A4/Mts1 relative to control mice ($P<0.05$) (Figure 5D). In contrast to previous reports,[23] we did not observe fragmentation of elastin with hypoxia, but this might reflect the level of vessel being assessed. In addition, in room air mice, we measured total lung elastin by desmosine radioimmunoassay and values were increased in S100A4/Mts1 versus the C57Bl/6 group ($P<0.001$) (Figure 5E), when normalized to body weight. Normalization of elastin in the central pulmonary artery or in the aorta to tissue segment rather than to total protein determines an absolute increase in elastin unobscured by elevation of other proteins in a hypertrophied organ,[19] but differences were not significant when normalizing the elastin to segment or to total protein (data not shown).

We determined whether the increased elastin could also be attributed to suppression of vascular elastase activity. Compared with a persistent steady-state lung elastase activity in control room air mice, an increase in elastase activity was noted in the C57Bl/6 mice after 2 days of hypoxia ($P<0.02$), that returned to control values by day 14 (Figure 5F). No significant increase in elastase activity relative to baseline was evident in S100A4/Mts1 mice after 2 days of hypoxia, but values were also not significantly different from C57Bl/6 mice at this time point. At 14 days after hypoxia, values in S100A4/Mts1 mice were reduced relative to C57Bl/6 mice ($P<0.01$).

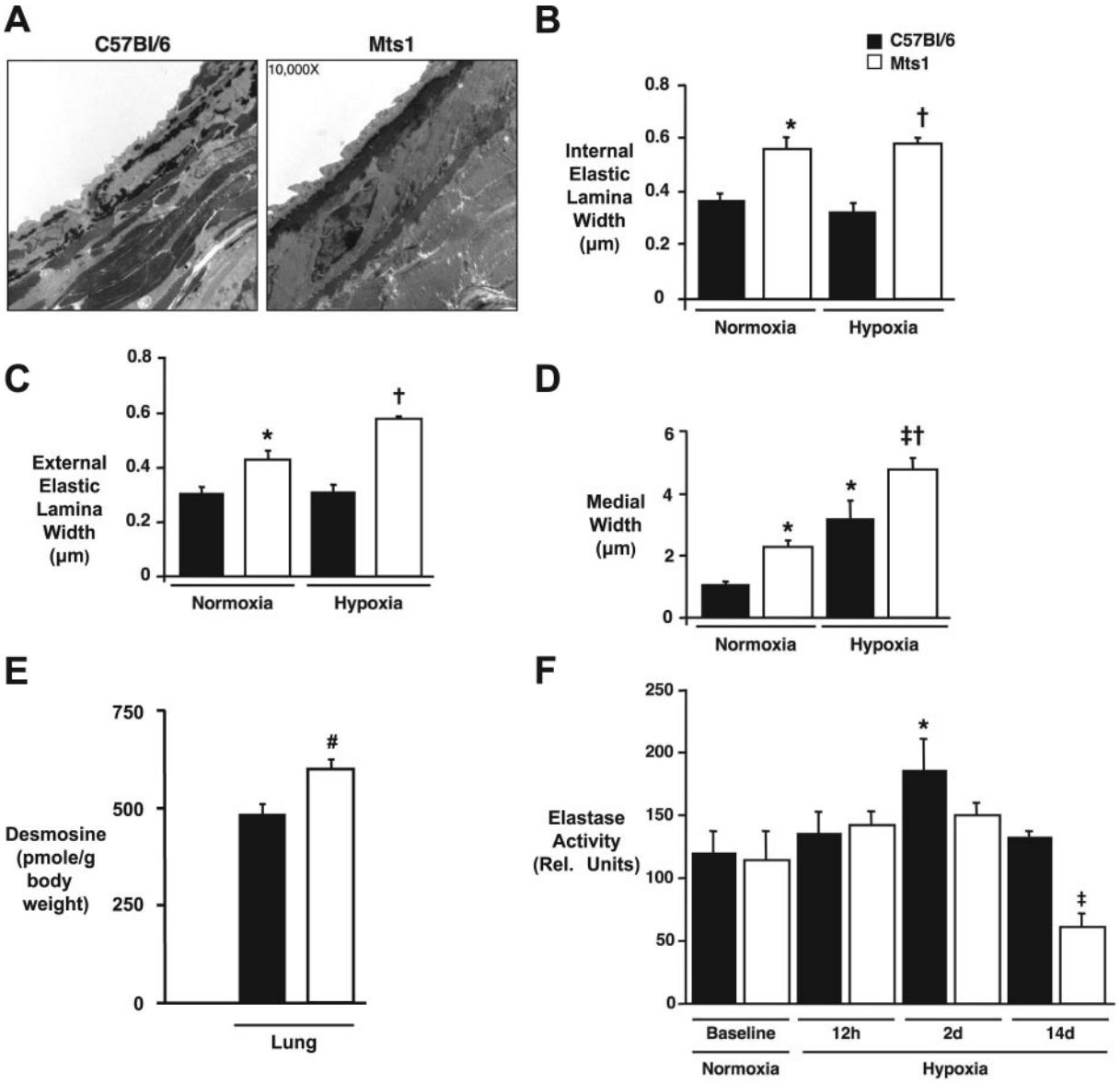

Figure 5. Elastin quantification, medial hypertrophy, and elastase activity. A, Representative electron photomicrographs of S100A4/Mts1 and C57Bl/6 PAs at the respiratory bronchiolus level (16 to 18 μm) as seen by transmission EM, at $\times$10 0000 magnification. Computed width of both the internal (B) and external (C) elastic laminae at baseline and in association with chronic hypoxia. D, Measurement of medial wall thickness as seen by EM. E, Desmosines were measured in whole lung of room air S100A4/Mts1 and C57Bl/6 mice and normalized per weight of the animal. F, Elastase activity in S100A4/Mts1 and C57Bl/6 mice exposed to room air or hypoxia at indicated time points. Elastase activity was assayed in triplicate from whole lung tissue using fluorogenic elastin. Data represent mean$\pm$SEM, (A through D, n=3; E, n=6; F, n=4 to 6); *$P<0.05$ compared with C57Bl/6 normoxic mice; †$P<0.05$ compared with C57Bl/6 hypoxic mice; ‡$P<0.05$ compared with S100A4/Mts1 normoxic mice; #$P<0.001$ compared with C57Bl/6 mice.

Discussion

S100A4/Mts1 mice had greater RVSP and RVH at baseline, in response to acute and chronic hypoxia, and after "recovery" in room air when compared with C57Bl/6 controls. Pulmonary vascular changes were, however, similar in both groups in room air and after chronic hypoxia, but regression was attenuated in the S100A4/Mts1 mice. We related these features to reduced cardiac function and to increased fibulin-5 and thicker elastic laminae, that could alter vascular tone, attenuate the severity of the vascular changes[21,22] expected for the level of pulmonary artery pressure and resistance,[24] and impair reversibility.

Our studies underscore the importance of considering the impact of altered cardiac function, on the pulmonary hypertensive phenotype. In severe PAH, the dilated RV can lead to impaired LV filling and reduced CO.[25] In the S100A4/Mts1 mice, a reduced CO accompanied a very mild elevation in RVSP. Thus, we pursued a load-independent assessment of cardiac function and documented reduced ventricular elastance through pressure-volume curves. The S100 family of calcium-binding proteins, are expressed in cardiac myocytes,[26] and although S100A4/Mts1 and S100A11 are elevated in response to myocardial injury,[27] their selective impact on cardiac function is not known. Although the

measurements of left ventricular dysfunction were made under anesthesia, all mice were similarly treated. In an attempt to further evaluate the cause of the impaired LV function, we assessed elastin in the aorta, but found no significant differences in S100A4/Mts1 versus control mice.

Although measurements were not made at the same time, the mildly elevated left ventricular end-diastolic pressure derived from the pressure volume loops might explain the increase in RVSP in the S100A4/Mts1 mice at baseline and in response to acute and chronic hypoxia. However, this would be unlikely to account for the lack of vasodilatation in response to nitric oxide or oxygen[28] and the failure to return to baseline levels of RVSP despite 3 months of "recovery" in room air. Thus we turned our attention to features that might explain a difference in vascular tone as well as attenuated remodeling relative to that expected for the elevation in PA pressure and estimated pulmonary vascular resistance.[24]

Normal assembly of elastin fibers prevents SMC proliferation,[22] and impaired elastin fiber assembly promotes this response.[21] In transgenic mice lacking the elastin gene, excess proliferation of SMCs was identified as causing occlusion of coronary arteries resulting in the animals' demise in the immediate postnatal period.[29] Along the same lines, our group has shown that there is degradation of elastin in the pathogenesis of pulmonary vascular disease,[19] and that elastase inhibitors can suppress smooth muscle cell proliferation, and associated pulmonary hypertension.[10,12,30] Thick elastic laminae, documented by electron microscopy, were associated with elevated desmosine levels in S100A4Mts1 versus control mice even in room air, and reduced elastase activity was documented in chronic hypoxia. It is interesting that the thick elastic laminae still permit hypertrophy of the SMCs during hypoxia, likely in response to the elevated pressure. Although these SMC were immunoreactive for alpha-smooth muscle actin, it would be interesting to assess other markers of differentiation. We could not document an increase in elastin in the large central pulmonary artery nor could we find a change in compliance in those vessels, suggesting that the features are limited to intraparenchymal vessels. Although the increase in elastin could have been related to airways in the lung tissue, this was not evident on microscopic analysis using a stain that recognizes elastin.

We speculate that in the S100A4/Mts1 mice, the increase in elastin limits the extent of abnormal muscularization of distal PAs,[24] by suppressing pericyte proliferation and differentiation to SMCs. Fibulin-5 stabilization of the elastic fibers, through its ability to promote cell attachment via cell surface integrins.[31] might also prevent endothelial cell apoptosis, accounting for reduced loss of vessels[32] relative to the elevation in pressure.[24] This feature could also repress smooth muscle apoptosis and regression of muscularization of distal vessels following return to room air. Only a tendency toward impaired "recovery" of the number of peripheral vessels was apparent in the S100A4/Mts1 compared with C57Bl/6 mice, but it is possible that the antiproliferative effect of elastin might also suppress the endothelial cell proliferation necessary for vascular regrowth. Lack of regression may, however, simply be a feature of failure of vasodilatation on return to room air.[33] We did not assess capillary surface area which is increased in hypoxia,[34] but our findings of loss of peripheral arteries is similar to that noted by other groups.[23]

Although there may be a link between lack of reversibility of vascular disease, and the propensity of a small subset of older S100A4/Mts1 mice to develop PVD,[5] we were unable to show that a "second hit" with chronic hypoxia induced these lesions (data not shown). It is possible that a different kind of insult or some property of aging is required.

Despite the reduced lumen diameter of the intrapulmonary arteries on microCT and the lack of vasodilation in response to NO or oxygen, we were unable to document that the increase in elastin correlated with a change in compliance of the large central PAs. A mouse hemizygous for elastin also showed normal compliance of these vessels,[29] so evaluation of the intrapulmonary arteries may be necessary to detect abnormalities.

Microarray studies also revealed genes that, in addition to fibulin-5, might be of further interest in explaining how S100A4/Mts1 could induce PVOD in the small subset of mice previously described.[5] For example, we observed a decrease in BMP-RI expression, in keeping with recent observations in lungs of patients with acquired idiopathic PAH.[35]

It is interesting that attenuation of vascular disease relative to the severity of pulmonary hypertension, is observed in the transgenic mouse with dominant negative[3] or haplo insufficiency BMP-RII.[4] Asymptomatic carriers of the idiopathic PAH disease haplotype (mutation in BMP-RII), have abnormally elevated PA systolic pressures in response to exercise,[36] but the structure of their pulmonary vessels is unknown.

In conclusion, our studies underscore the complexity of determining how environmental and genetic factors ultimately lead to the development of PVD. The low penetrance of BMP-RII abnormalities in producing severe disease,[1,2] may be related to our observation that altered expression of a gene can trigger a compensatory mechanism. It is, perhaps, through understanding why these compensatory mechanisms fail, that we will identify critical risk factors and modifier genes that can be targeted in developing new approaches to treatment.

Acknowledgments

Supported by grant number 1-R01-HL074186-01 from the National Institutes of Health and the Dwight and Vera Dunlevie Endowed Professorship to M.R. S.M. was supported in part by a University of Toronto Fellowship. E.S. was supported by a fellowship from the American Heart Association/Pulmonary Hypertension Association.

References

1. Lane KB, Machado RD, Pauciulo MW, Thomson JR, Phillips JA 3rd, Loyd JE, Nichols WC, Trembath RC. Heterozygous germline mutations in BMPR2, encoding a TGF-beta receptor, cause familial primary pulmonary hypertension. The International PPH Consortium. *Nat Genet*. 2000;26:81–84.
2. Deng Z, Morse JH, Slager SL, Cuervo N, Moore KJ, Venetos G, Kalachikov S, Cayanis E, Fischer SG, Barst RJ, Hodge SE, Knowles JA. Familial primary pulmonary hypertension (gene PPH1) is caused by mutations in the bone morphogenetic protein receptor-II gene. *Am J Hum Genet*. 2000;67:737–744.
3. West J, Fagan K, Steudel W, Fouty B, Lane K, Harral J, Hoedt-Miller M, Tada Y, Ozimek J, Tuder R, Rodman DM. Pulmonary hypertension in

transgenic mice expressing a dominant-negative BMPRII gene in smooth muscle. *Circ Res*. 2004;94:1109–1114.
4. Beppu H, Ichinose F, Kawai N, Jones RC, Yu PB, Zapol WM, Miyazono K, Li E, Bloch KD. BMPR-II heterozygous mice have mild pulmonary hypertension and an impaired pulmonary vascular remodeling response to prolonged hypoxia. *Am J Physiol Lung Cell Mol Physiol*. 2004;287: L1241–L1247.
5. Greenway S, van Suylen RJ, Du Marchie Sarvaas G, Kwan E, Ambartsumian N, Lukanidin E, Rabinovitch M. S100A4/Mts1 produces murine pulmonary artery changes resembling plexogenic arteriopathy and is increased in human plexogenic arteriopathy. *Am J Pathol*. 2004;164: 253–262.
6. Albertazzi E, Cajone F, Leone BE, Naguib RN, Lakshmi MS, Sherbet GV. Expression of metastasis-associated genes h-mts1 (S100A4) and nm23 in carcinoma of breast is related to disease progression. *DNA Cell Biol*. 1998;17:335–342.
7. Kriajevska M, Tarabykina S, Bronstein I, Maitland N, Lomonosov M, Hansen K, Georgiev G, Lukanidin E. Metastasis-associated Mts1 (S100A4) protein modulates protein kinase C phosphorylation of the heavy chain of nonmuscle myosin. *J Biol Chem*. 1998;273:9852–9856.
8. Ambartsumian N, Klingelhofer J, Grigorian M, Christensen C, Kriajevska M, Tulchinsky E, Georgiev G, Berezin V, Bock E, Rygaard J, Cao R, Cao Y, Lukanidin E. The metastasis-associated Mts1(S100A4) protein could act as an angiogenic factor. *Oncogene*. 2001;20:4685–4695.
8a. Lawrie A, Spiekerkoetter E, Martinez EC, Ambartsumian N, Sheward WJ, MacLean MR, Harmar AJ, Schmidt AM, Lukanidin E, Rabinovitch M. Interdependent serotonin transporter and receptor pathways regulate S100A4/Mts1, a gene associated with pulmonary vascular disease. *Circ Res.* 2005;97:227–235.
9. Ambartsumian N, Klingelhofer J, Grigorian M, Karlstrom O, Sidenius N, Georgiev G, Lukanidin E. Tissue-specific posttranscriptional downregulation of expression of the S100A4(mts1) gene in transgenic animals. *Invasion Metastasis*. 1998;18:96–104.
10. Zaidi SH, You XM, Ciura S, Husain M, Rabinovitch M. Overexpression of the serine elastase inhibitor elafin protects transgenic mice from hypoxic pulmonary hypertension. *Circulation*. 2002;105:516–521.
11. Rabinovitch M, Andrew M, Thom H, Trusler GA, Williams WG, Rowe RD, Olley PD. Abnormal endothelial factor VIII associated with pulmonary hypertension and congenital heart defects. *Circulation*. 1987;76: 1043–1052.
12. Ye CL, Rabinovitch M. Inhibition of elastolysis by SC-37698 reduces development and progression of monocrotaline pulmonary hypertension. *Am J Physiol*. 1991;261:H1255–H1267.
13. Faury G, Pezet M, Knutsen RH, Boyle WA, Heximer SP, McLean SE, Minkes RK, Blumer KJ, Kovacs A, Kelly DP, Li DY, Starcher B, Mecham RP. Developmental adaptation of the mouse cardiovascular system to elastin haploinsufficiency. *J Clin Invest*. 2003;112:1419–1428.
14. Georgakopoulos D, Mitzner WA, Chen CH, Byrne BJ, Millar HD, Hare JM, Kass DA. In vivo murine left ventricular pressure-volume relations by miniaturized conductance micromanometry. *Am J Physiol*. 1998;274: H1416–H1422.
15. Tabibiazar R, Wagner RA, Liao A, Quertermous T. Transcriptional profiling of the heart reveals chamber-specific gene expression patterns. *Circ Res*. 2003;93:1193–1201.
16. Yanagisawa H, Davis EC, Starcher BC, Ouchi T, Yanagisawa M, Richardson JA, Olson EN. Fibulin-5 is an elastin-binding protein essential for elastic fibre development in vivo. *Nature*. 2002;415: 168–171.
17. Hinek A, Mecham RP, Keeley F, Rabinovitch M. Impaired elastin fiber assembly related to reduced 67-kD elastin-binding protein in fetal lamb ductus arteriosus and in cultured aortic smooth muscle cells treated with chondroitin sulfate. *J Clin Invest*. 1991;88:2083–2094.
18. Starcher B. A ninhydrin-based assay to quantitate the total protein content of tissue samples. *Anal Biochem*. 2001;292:125–129.
19. Todorovich-Hunter L, Dodo H, Ye C, McCready L, Keeley FW, Rabinovitch M. Increased pulmonary artery elastolytic activity in adult rats with monocrotaline-induced progressive hypertensive pulmonary vascular disease compared with infant rats with nonprogressive disease. *Am Rev Respir Dis*. 1992;146:213–223.
20. Nakamura T, Lozano PR, Ikeda Y, Iwanaga Y, Hinek A, Minamisawa S, Cheng CF, Kobuke K, Dalton N, Takada Y, Tashiro K, Ross J Jr, Honjo T, Chien KR. Fibulin-5/DANCE is essential for elastogenesis in vivo. *Nature*. 2002;415:171–175.
21. Urban Z, Riazi S, Seidl TL, Katahira J, Smoot LB, Chitayat D, Boyd CD, Hinek A. Connection between elastin haploinsufficiency and increased cell proliferation in patients with supravalvular aortic stenosis and Williams-Beuren syndrome. *Am J Hum Genet*. 2002;71:30–44.
22. Karnik SK, Brooke BS, Bayes-Genis A, Sorensen L, Wythe JD, Schwartz RS, Keating MT, Li DY. A critical role for elastin signaling in vascular morphogenesis and disease. *Development*. 2003;130:411–423.
23. Levi M, Moons L, Bouche A, Shapiro SD, Collen D, Carmeliet P. Deficiency of urokinase-type plasminogen activator-mediated plasmin generation impairs vascular remodeling during hypoxia-induced pulmonary hypertension in mice. *Circulation*. 2001;103:2014–2020.
24. Rabinovitch M, Gamble W, Nadas AS, Miettinen OS, Reid L. Rat pulmonary circulation after chronic hypoxia: hemodynamic and structural features. *Am J Physiol*. 1979;236:H818–H827.
25. Marcus JT, Vonk Noordegraaf A, Roeleveld RJ, Postmus PE, Heethaar RM, Van Rossum AC, Boonstra A. Impaired left ventricular filling due to right ventricular pressure overload in primary pulmonary hypertension: noninvasive monitoring using MRI. *Chest*. 2001;119:1761–1765.
26. Tsoporis JN, Marks A, Zimmer DB, McMahon C, Parker TG. The myocardial protein S100A1 plays a role in the maintenance of normal gene expression in the adult heart. *Mol Cell Biochem*. 2003;242:27–33.
27. Inamoto S, Murao S, Yokoyama M, Kitazawa S, Maeda S. Isoproterenol-induced myocardial injury resulting in altered S100A4 and S100A11 protein expression in the rat. *Pathol Int*. 2000;50:480–485.
28. Adatia I, Perry S, Landzberg M, Moore P, Thompson JE, Wessel DL. Inhaled nitric oxide and hemodynamic evaluation of patients with pulmonary hypertension before transplantation. *J Am Coll Cardiol*. 1995;25: 1656–1664.
29. Li DY, Brooke B, Davis EC, Mecham RP, Sorensen LK, Boak BB, Eichwald E, Keating MT. Elastin is an essential determinant of arterial morphogenesis. *Nature*. 1998;393:276–280.
30. Maruyama K, Ye CL, Woo M, Venkatacharya H, Lines LD, Silver MM, Rabinovitch M. Chronic hypoxic pulmonary hypertension in rats and increased elastolytic activity. *Am J Physiol*. 1991;261:H1716–H1726.
31. Nakamura T, Ruiz-Lozano P, Lindner V, Yabe D, Taniwaki M, Furukawa Y, Kobuke K, Tashiro K, Lu Z, Andon NL, Schaub R, Matsumori A, Sasayama S, Chien KR, Honjo T. DANCE, a novel secreted RGD protein expressed in developing, atherosclerotic, and balloon-injured arteries. *J Biol Chem*. 1999;274:22476–22483.
32. Zhao YD, Campbell AI, Robb M, Ng D, Stewart DJ. Protective role of angiopoietin-1 in experimental pulmonary hypertension. *Circ Res*. 2003; 92:984–991.
33. O'Blenes SB, Fischer S, McIntyre B, Keshavjee S, Rabinovitch M. Hemodynamic unloading leads to regression of pulmonary vascular disease in rats. *J Thorac Cardiovasc Surg*. 2001;121:279–289.
34. Howell K, Preston RJ, McLoughlin P. Chronic hypoxia causes angiogenesis in addition to remodelling in the adult rat pulmonary circulation. *J Physiol*. 2003;547:133–145.
35. Du L, Sullivan CC, Chu D, Cho AJ, Kido M, Wolf PL, Yuan JX, Deutsch R, Jamieson SW, Thistlethwaite PA. Signaling molecules in nonfamilial pulmonary hypertension. *N Engl J Med*. 2003;348:500–509.
36. Grunig E, Janssen B, Mereles D, Barth U, Borst MM, Vogt IR, Fischer C, Olschewski H, Kuecherer HF, Kubler W. Abnormal pulmonary artery pressure response in asymptomatic carriers of primary pulmonary hypertension gene. *Circulation*. 2000;102:1145–1150.

Circulation Research
JOURNAL OF THE AMERICAN HEART ASSOCIATION

Increased Fibulin-5 and Elastin in S100A4/Mts1 Mice With Pulmonary Hypertension

Sandra L. Merklinger, Roger A. Wagner, Edda Spiekerkoetter, Aleksander Hinek, Russell H. Knutsen, M. Golam Kabir, Kavin Desai, Shelby Hacker, Lingli Wang, Gordon M. Cann, Noona S. Ambartsumian, Eugene Lukanidin, Daniel Bernstein, Mansoor Husain, Robert P. Mecham, Barry Starcher, Hiromi Yanagisawa and Marlene Rabinovitch

Circ Res. 2005;97:596-604; originally published online August 18, 2005;
doi: 10.1161/01.RES.0000182425.49768.8a
Circulation Research is published by the American Heart Association, 7272 Greenville Avenue, Dallas, TX 75231

Print ISSN: 0009-7330. Online ISSN: 1524-4571

Online Table 1

Final body weight, mean arterial pressure, hematocrit and cardiac output measurements

		FBW (g)	MAP (mmHg)	Hematocrit (%)	Cardiac Output (ml/min)
Normoxia	C57Bl/6	24±1.8	74.8±2.9	42.2±0.4	17.5±2.6
	S100A4/Mts1	24.5±1.1	70±3.7	43.3±0.5	12±2.0*
Hypoxia	C57Bl/6	20.4±1.2	63±2.1*	61.3±0.4*	22.1±2.5
	S100A4/Mts1	17.6±1.1‡	64±2.6‡	62.6±1.3*	14±0.8†

FBW indicates final body weight. MAP indicates mean arterial blood pressure.

*P<0.0001 compared to C57Bl/6 normoxia; †P<0.01 compared to C57Bl/6 hypoxia; ‡P<0.002 compared to S100A4/Mts1 normoxia.

Online Table 2

Heart rate, end-diastolic pressure and dP/dt obtained from pressure/volume loops

	Heart Rate	End-Diastolic Pressure, (mmHg)	dP/dt_{max} (mmHg/s)	dP/dt_{min} (mmHg/s)
C57Bl/6	344±11.1	3.9±0.2	6591±428	-4884±485
S100A4/Mts1	356±13.3	7.7±1.6*	5428±554	-4792±606

*P<0.05 compared to C57Bl/6 mice.

Online Table 3

Selected microarray data for S100A4/Mts1 vs. Control C57Bl/6 mice after chronic hypoxia

Function	Elevated Gene	Fold Increase
Proteases	Matrix metalloproteinase 2	1.58
Matrix	* Fibulin-5	1.21
Growth	** Tumor necrosis factor-α	1.31
	** Stromal-derived factor 1	1.41
	* Ephrin receptor B6	1.35
Vasoreactive	* Endothelin 3	1.11
	† Prostaglandin Synthase	1.23

*Trend by qRT-PCR, **Significant by qRT-PCR ($P<0.05$),

†Not confirmed by qRT-PCR.